Approaching classicality in quantum accelerator modes through decoherence

M. B. d'Arcy, R. M. Godun, M. K. Oberthaler,* G. S. Summy, and K. Burnett
Clarendon Laboratory, Department of Physics, University of Oxford, Parks Road, Oxford OX1 3PU, United Kingdom

S. A. Gardiner
Institut für Physik, Universität Potsdam, Am Neuen Palais 10, D-14469 Potsdam, Germany
and Institut für Theoretische Physik, Universität Hannover, Appelstraße 2, D-30167 Hannover, Germany
(Received 23 November 2000; revised manuscript received 7 August 2001; published 30 October 2001)

We describe measurements of the mean energy of an ensemble of laser-cooled atoms in an atom optical system in which the cold atoms, falling freely under gravity, receive approximate δ-kicks from a pulsed standing wave of laser light. We call this system a ''δ-kicked accelerator.'' Additionally, we can counteract the effect of gravity by appropriate shifting of the position of the standing wave, which restores the dynamics of the standard δ-kicked rotor. The presence of gravity (δ-kicked accelerator) yields quantum phenomena, quantum accelerator modes, which are markedly different from those in the case for which gravity is absent (δ-kicked rotor). Quantum accelerator modes result in a much higher rate of increase in the mean energy of the system than is found in its classical analog. When gravity is counteracted, the system exhibits the suppression of the momentum diffusion characteristic of dynamical localization. The effect of noise is examined and a comparison is made with simulations of both quantum-mechanical and classical versions of the system. We find that the introduction of noise results in the restoration of several signatures of classical behavior, although significant quantum features remain.

DOI: 10.1103/PhysRevE.64.056233 PACS number(s): 05.45.Mt, 32.80.Pj, 42.50.Vk, 72.15.Rn

I. INTRODUCTION

The consensus of theoretical investigations into chaotic systems has been that many effects peculiar to classical chaos (e.g., exponential divergence in phase space of paths beginning in close proximity) are no longer observable in a quantum system [1,2]. The challenge has been to observe which aspects of characteristically chaotic behavior do persist in the quantum case, and hence to establish the characteristics of ''quantum chaos,'' thus defining more carefully what such a concept means. Furthermore, if the behavior of the quantum system can be made to resemble more closely that of a theoretical classical system (in terms of its momentum distribution and variation of mean energy with time) then it is possible to investigate quantum-classical correspondence and how the observed classical behavior in nature has its origin in the quantum domain. In the case of classically chaotic systems this correspondence cannot be made using the semiclassical Bohr-Sommerfeld [3,4] or Einstein-Brillouin-Keller [5–8] quantization schemes that are appropriate for systems with more than one degree of freedom [9].

In this paper, we utilize an atom optical system in which cold trapped atoms are released and periodically kicked with a vertically oriented, spatially periodic potential created by a standing wave of laser light. This δ-kicked accelerator is equivalent to a realization of the δ-kicked rotor [10] with an additional linear potential due to gravity. This can markedly alter the behavior of the system, resulting in, for example, quantum accelerator modes [11].

We study the variation in the mean energy of the atoms. This quantity is useful in characterizing the behavior of the system because its variation is considerably different depending on whether the system is classical or quantum mechanical. We also introduce noise through induced spontaneous emission, and find that the noise results in the restoration of a classical-like variation in the mean energy of the atoms; the same level of noise produces little modification to the gross behavior of the corresponding classical system. By consideration of the system's behavior in the presence of noise, we discuss the extent to which this can be viewed as being more classical. We find good qualitative agreement between experimental results and numerical simulations.

In Sec. II we summarize the theoretical background to this investigation and the motivation for undertaking it. In Sec. III we explain our experimental and numerical methods, and in Sec. IV we present and discuss our results.

II. MOTIVATION

Due in particular to the ease of integrating the equations of motion [12–15], a great deal of theoretical study of chaotic dynamics, both classical and quantum mechanical, has been carried out on one-dimensional integrable systems perturbed by a periodic train of position-dependent kicks, ''δ-kicks,'' whose time dependence is described by a δ function. Experimentally accessible atom optical systems are, within certain parameter regimes, capable of closely emulating such idealized dynamics, and thus provide a direct check for theoretical and numerical predictions.

We have achieved an atom optical realization of such a system, the δ-kicked accelerator, the relevant dynamics of which can be described by the following Hamiltonian:

$$\hat{H}=\frac{\hat{p}^2}{2m}+mg\hat{x}+\frac{I_{\max}}{G}[1+\cos(G\hat{x})]\sum_N \delta(t-NT), \quad (1)$$

*Present address: Universität Konstanz, Fachbereich Physik, Universitätsstraße 10, D-78457 Konstanz, Germany.

where $\hat{x}$ is the position operator, $\hat{p}$ is the momentum operator, m is the particle mass, g is the gravitational acceleration of free fall, $I_{\max}$ is the magnitude of the maximum possible impulse received by a *classical* point particle, $G = 2\pi/\lambda_{\text{spat}}$, where λ_{spat} is the spatial period of the potential, t is the time, T is the time interval between applications of the potential (the ''pulse period''), and N is the kick number. Note that we use a caret to denote *operator* quantities, so that, for example, $\hat{x}$ is the operator corresponding to the classical position x.

The time evolution of the system can be described in discrete steps corresponding to successive applications of the kicks, producing a kick-to-kick mapping. We use a convenient choice of rescaled effective position and momentum variables, $\chi = Gx$ and $\rho = GTp/m$, to arrive at the classical mapping

$$\rho_{n+1} = \rho_n + K\sin(\chi_n) - \gamma, \tag{2}$$

$$\chi_{n+1} = \chi_n + \rho_{n+1} + \frac{\gamma}{2}. \tag{3}$$

We see that there are only two free parameters, $K = I_{\max}GT/m$ and $\gamma = gGT^2$, and if we set $\gamma = 0$, we regain the standard map, corresponding to the dynamics of the usual δ-kicked rotor [12], in which K is simply the classical stochasticity parameter. In our experimental configuration it is possible to effectively vary γ independently of K, so that we can (in an accelerating frame) realize simple δ-kicked rotor dynamics [16,17].

In the quantum-mechanical case we can integrate the corresponding Schrödinger equation over the interval between two successive kicks. We thus arrive at $|\psi_{n+1}\rangle = \hat{U}|\psi_n\rangle$ where $|\psi_n\rangle$ is the wave function just prior to the application of the $(n+1)$th kick, and $\hat{U}$ is the Floquet operator,

$$\hat{U} = \exp[-i(\gamma\hat{\chi} + \hat{\rho}^2/2)/\tau]\exp[-iK\{1+\cos(\hat{\chi})\}/\tau]. \tag{4}$$

The Floquet operator describes the wave-mechanical equivalent of the classical mapping of Eqs. (2) and (3); note that in addition to K and γ, the quantum evolution depends on the parameter $\tau = \hbar G^2 T/m = -i[\hat{\chi}, \hat{\rho}]$, which is effectively a scaled Planck constant. It is possible to regard the effect of the kicking potential on the incident de Broglie waves as being equivalent to that of a phase diffraction grating. The amplitude of the variation (with position) of the induced phase shift is $\phi_d = K/\tau$, which is the maximum classical impulse in units of grating recoils, i.e., $\phi_d = I_{\max}/(\hbar G)$.

Due to the spatially and temporally periodic nature of the system, phase space is also periodic. Thus classically one need consider only initial conditions such that $-\pi < \chi_i \leqslant \pi$ and $-\pi < \rho_i \leqslant \pi$, as these encompass all possible types of dynamical behavior. Quantum mechanically, initial plane waves whose values of ρ differ by 2π respond identically to the diffractive effect of the kicking potential. Any momentum of an initial plane wave is equivalent to a momentum in this range, known as a *quasimomentum*. This is similar to the situation in solid state physics in which any Bloch state is equivalent to the one whose wave vector differs from that of the first by an integer number of reciprocal lattice vectors and lies in the first Brillouin zone [18,19]. This property is due to the spatial periodicity of the system.

In the case of the δ-kicked rotor (i.e., $\gamma = 0$), when $K \ll 1$ the classical motion of the system is predominantly regular and the majority of this classical phase space consists of stable regions. Any momentum diffusion of an initial ensemble of particles is greatly restricted due to numerous Kol'mogorov-Arnol'd-Moser (KAM) tori [55–57], which form barriers in phase space through which trajectories may not pass [12]. As K is increased, the KAM tori progressively break up, and the proportion of phase space exhibiting stochastic behavior increases, leading to a much greater possibility of momentum diffusion. As discussed in Ref. [12], for $K > 0.971\,64$, momentum increase to arbitrarily large values is possible and the behavior is globally chaotic. When $K \gg 1$ the behavior of the momentum distribution of the system is well characterized by random walk diffusion, so the mean energy of the system will increase linearly with kick number. The diffusive behavior is not as a result of any randomness in the force but is due to the pseudorandom behavior characteristic of chaotic dynamics. It can, like any diffusion, be characterized by a diffusion parameter, in general $D(K,\gamma)$. Although the global behavior of the system is dependent only on the stochasticity parameter K, the precise behavior of individual particles depends also on their initial conditions. It is, for example, possible for certain particles to fulfil the condition for linear momentum increase by being in the correct position at the instant of every kick so as to receive the maximum possible impulse. Such particles are in an accelerator mode [12], and in phase space are to be found in small islands, localized around the values of x for which the potential gradient is maximum. Their energy increases as N^2, so that the mean energy of an ensemble of particles can be described by

$$E(N) = D(K,\gamma)N^{\alpha}, \tag{5}$$

where α is a little more than 1. The system is said to exhibit anomalous diffusion whenever α differs from 1 (when $\alpha > 1$ the energy growth is superdiffusive; when $\alpha < 1$ the growth is subdiffusive: it is, for example, possible for consecutive kicks to cancel out each other's effect for certain initial conditions).

The behavior of the quantum system is radically different from that of its classical counterpart and numerous theoretical investigations concerning it have been made. The most celebrated aspect of this quantum behavior is dynamical localization. This was first discovered numerically [16], and subsequently explained by analogy with the phenomenon of Anderson localization of electronic states in random lattices [20,21]. The effects of dynamical localization were first observed experimentally in microwave ionization of hydrogen atoms [22,23], and dynamical localization itself was first observed directly by Moore *et al.* [24] in an atom optical system.

When the δ-kicks are applied, the mean energy at first increases diffusively, i.e., linearly with kick number, as in the classical system. Provided that τ is not a rational multiple of 4π [13,25], this diffusive behavior only persists for a finite number of kicks, the so-called quantum break time. Beyond this, the mean energy of the system no longer increases; the classical diffusion has been quantum mechanically suppressed. The final momentum distribution of the ensemble displays a symmetric exponential form whose fall-off is characterized by the localization length [20]. The spectrum of quasienergies associated with the Floquet states (i.e., the eigenvalues associated with the eigenstates of the Floquet operator) is discrete, and the Floquet states themselves are exponentially localized and separated in momentum space. Momentum diffusion is thus limited by the extent in momentum space of those Floquet states that are initially occupied.

When $\tau=4\pi a/b$, where a and b are integers, the spectrum of quasienergy states is absolutely continuous and the system exhibits a so-called quantum resonance [13,25,26] of order b. This is characterized by a momentum distribution that is nonexponential in form, and in which dynamical localization does not occur. Instead, for certain initial values of quasimomenta quadratic growth in the energy with kick number occurs in the limit of a large number of kicks. The values of the quasimomentum for which this quadratic growth occurs depend on the value of τ. For all other quasimomenta we observe numerically that the mean energy oscillates with kick number. The amplitude and period of these oscillations grow as the initial quasimomentum approaches one of the resonant values for which unbounded quadratic growth can occur. Since the ensemble consists of a continuous range of initial momenta that exhibit these different types of energy-growth behavior as kicks are applied, the growth in the mean energy of the ensemble as a whole is linear in the limit of a large number of kicks [27].

For the δ-kicked accelerator ($\gamma\neq 0$), the behavior is dramatically modified for certain values of τ. Quantum accelerator modes [11] appear, characterized by a linear increase in the momentum along the axis of the external force of a portion of the ensemble of quantum-mechanical particles as pulses are applied. This leads to a pronounced asymmetric momentum distribution and as such constitutes an easily observed quantum effect. In the diffractive picture the effect of the kicking potential is to diffract the wave function into different momentum states, as discussed in Ref. [28]. Those which rephase after subsequent kicks determine the momentum of the accelerator mode. The presence of gravity allows a small number of states with progressively larger values of momentum to rephase just before the next kick is applied.

Any experimental configuration can only approximate a δ-kicked system because real kicks must be of finite duration. For sufficiently short kicks and particles (in our case cold caesium atoms) of sufficiently low absolute velocity, this distinction is unimportant (this will be discussed further in Sec. III A). A practical realization is also susceptible to noise, ignored in an ideal system. Noise may be due to factors such as vibrations of the apparatus, variation in time of the applied potential, or spontaneous emission of the atoms. We can achieve a system that is approximately ideal by minimizing these effects. On the other hand, if we can control the noise levels we can investigate systematically any modifications in behavior. In particular, the presence of a quantifiable level of noise could be useful in attempting to investigate the role of coherence in a system and to what extent, if any, a quantum system can be regarded as being more classical if the coherence is perturbed. From a classical viewpoint, the noise introduces a random component [29] into the momentum incrementation of the standard mapping, with consequent modification to the diffusion parameter. In the quantum case, noise also disturbs the coherence of the wave function. When the noise is weak compared with the kicking strength, the classical motion is only slightly affected, whereas the quantum-mechanical motion is significantly modified, in that signatures of characteristically quantum behavior, such as dynamical localization, are degraded. We emphasize that we are not discussing the case where noise dominates the energy growth, either in the classical system or in the quantum system [30]. We also note that, even with the degradation of particular signatures of quantum behavior, the system cannot be regarded as being truly classical since we do not approach the limit $\hbar\rightarrow 0$, which is a necessary (though not, it has been argued [31], sufficient) condition for a system to behave classically.

There have been both theoretical [29,30,32,33] and experimental [34–40] investigations of the effect of noise. The most important result of these is that the diffusive behavior of the system is modified so that the momentum diffusion is no longer zero after the quantum break time. Any diffusion that takes place after the quantum break time will henceforth be referred to as ''quantum diffusion,'' following the convention established by Ammann *et al.* [35], who argue that this diffusion is not accounted for by classical behavior of the system but by a modification of the quantum-mechanical behavior in the zero-diffusion case. These previous investigations lead us to examine further the effect of noise in modifying the behavior of our system, particularly with respect to quantum accelerator modes, which constitute a pronounced quantum effect peculiar to the $\gamma\neq 0$ case.

III. METHODS OF INVESTIGATION

A. Experimental methods

The first experimental investigations of quantum chaos [22,23,41,42] studied the microwave excitation and ionization of excited hydrogen atoms. Observation of the coherence-destroying effects of noise [34] used similar techniques involving Rydberg states of rubidium atoms. More recently, atom optical approaches have yielded almost exact realizations of the δ-kicked rotor [10,11,28,35–40,43–45]; this has the great benefit of allowing investigation of the extensive theoretical predictions available for this paradigmatic system. The configuration used in the current experiment is a slight modification of that described in our previous work [11,28].

Our apparatus consists of a glass vacuum cell in which we create a magneto-optic trap (MOT) for caesium atoms (whose mass m is 2.209×10^{-25} kg). A schematic diagram of the experimental configuration is shown in Fig. 1. Typically,

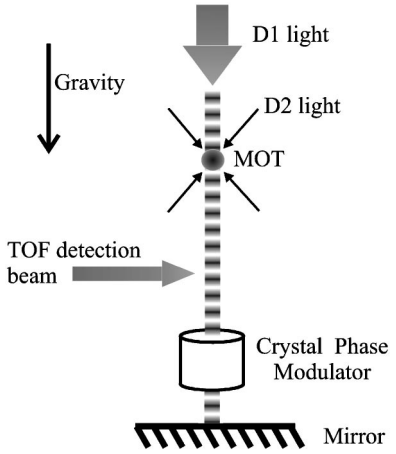

FIG. 1. Schematic diagram of the experimental arrangement. The time of flight (TOF) measurement of the atomic momentum distribution is made 50 cm below the MOT, and the crystal phase modulator allows the atoms to experience different effective gravitational accelerations.

a trap consists of 10^6 atoms and is ~ 2 mm in diameter. The trapping and molasses cooling use the $D2$ $(6^2S_{1/2} \rightarrow 6^2P_{3/2})F=4 \rightarrow F''=5$ transition (we denote hyperfine states of the $6^2S_{1/2}$ level by F, those of the $6^2P_{1/2}$ level by F', and those of the $6^2P_{3/2}$ level by F''). The atoms' distribution in momentum is then Gaussian, centered around zero and with a full width at half maximum (FWHM) of $12\hbar k_2$ (where $k_2=7.374\times 10^6$ m^{-1} is the wave vector of the $D2$ light), corresponding to a temperature of 5 μK. The potential that the atoms experience is produced by the application of a standing wave of light from a Ti:sapphire laser that is 30 GHz red detuned from the $D1$ $(6^2S_{1/2} \rightarrow 6^2P_{1/2})F=4 \rightarrow F'=3$ transition. The $D1$ light is passed through an acousto-optic modulator (AOM) and the emergent first order is delivered to the vacuum system via an optical fiber and optics that ensure that the light is linearly polarized. The light is then directed vertically downwards through the cell, parallel to the gravitational acceleration, and is retroreflected to produce a standing wave. Before and after retroreflection, the light is passed through a crystal phase modulator; this can produce a shift in the position of the standing wave between two consecutive $D1$ light pulses such that, in the frame of reference of a falling atom, the standing wave appears in the position expected if there were no gravitational field.

The AOM allows the light to be flashed on periodically with a pulse duration of $t_p=500$ ns and a shape that is approximately rectangular in form. The maximum power delivered to the vacuum system during this pulse is ~ 350 mW. Due to fluctuations in the power emerging from the Ti:sapphire laser and in the polarization of the $D1$ light coming out of the fiber before entering the polarization-maintaining optics, the power delivered to the system can vary by $\pm 5\%$ over the time scale of the experiment, while the detuning can vary by ~ 100 MHz (i.e., 0.3%). Passage through the phase modulator results in a narrowing of the beam and an overall loss of power. Fitting a Gaussian to the retroreflected beam profile, we estimate the waist of the resulting standing wave to be ~ 1.0 mm (FWHM) in the region of the MOT. Additional power losses occur at the retroreflecting mirror and the windows of the vacuum system. Taking all of this into account, we estimate the power in the retroreflected beam, when incident on the atoms in the MOT, to be ~ 120 mW and hence the maximum intensity experienced by atoms in the standing wave to be $I_0 \sim 1\times 10^8$ mW/cm^2. The time between consecutive pulses can be varied from 6 μs to 210 μs. The sequence of $D1$ light pulses is applied 5.2 ms after the end of molasses cooling and lasts for, at most, 6.3 ms. The steady-state spontaneous emission rate of atoms in a far-detuned light field is given by $R=\Omega^2\Gamma/4\delta_L^2$ [46], where Ω is the Rabi frequency of the atoms in the field, Γ is the linewidth of the transition, and δ_L is the detuning of the light from this transition. In this case, since the red detuning of the $D1$ light from resonance is 30 GHz, the mean number of spontaneous emissions for each atom over the time of one pulse is less than 2×10^{-3}. The atoms are then allowed to fall 50 cm under gravity to a point where they pass through a sheet of on-resonant $D2$ light. A time of flight (TOF) technique, in which the transmitted intensity of this light is measured by photodiodes as a function of time, is used to establish the momentum distribution of the atoms. The output signal from the photodiodes is passed through a lock-in amplifier, whose reference signal is at 40 kHz, in order to increase the signal-to-noise ratio. Since the typical width of an absorption signal is ~ 10 ms, the dither frequency is sufficiently high to allow resolution of all its features. The time constant of the lock-in amplifier's low-pass filter is 1 ms, and this finite bandwidth causes some distortion of narrow measured distributions. This leads to an apparent asymmetry and consequent increased width. For example, a distribution whose true width is $12\hbar k_2$ has an apparent width due to the lock-in amplifier of $12.5\hbar k_2$, and the high-momentum half-width exceeds the low-momentum half-width by $\sim 8\%$. The asymmetry and width increase are less pronounced for wider distributions (i.e., those with smaller high-frequency components).

The energy of an atom is shifted by an amount determined, through the light shift, by the intensity and detuning of the $D1$ light in which the atom finds itself. Thus the standing light wave creates a spatially varying sinusoidal potential for the atoms, in which the maximum Rabi frequency Ω_0 is given by $\Omega_0^2=\Gamma_1^2 I_0/I_{\rm sat}$, where $\Gamma_1=(2\pi)4.55$ MHz is the $D1$ transition linewidth, and $I_{\rm sat}=1.66$ mW/cm^2 is the saturation intensity of this transition. For a sufficiently large detuning δ_L, the excited state amplitude can be adiabatically eliminated [47,48]. If we then regard the short pulses as being approximate δ-kicks, the maximum impulse, which the standing wave can deliver classically to an atom, is given by $I_{\rm max}=\hbar\Omega_0^2 G t_p/(4\delta_L)$, where $G=2k_1$, and $k_1=7.025\times 10^6$ m^{-1} is the wave vector of the $D1$ light. We are justified in making the δ-function approximation (and ascribing the impulse delivered by the finite-duration pulse to that of an instantaneous δ-function) provided that the atoms do not move a distance comparable with the period of the standing wave during the time for which the light is on. In this case any averaging over the spatial variation of the potential, due to movement of the atoms during the time for which the

pulse is applied, is negligible. An atom that fulfils this criterion is said to be in the Raman-Nath regime. Outside this regime, the finite pulse duration causes the effective value of the stochasticity parameter to be reduced as the atomic velocity increases [45]. In our experiment, the momenta attained by the atoms were such that, in general, the Raman-Nath condition was imperfectly fulfilled but the degree of averaging over the potential was sufficiently small that the behavior observed was still characteristic of a δ-kicked system, albeit one with a reduced stochasticity parameter. Only in those cases where the atoms attained the very highest momenta (see Sec. IV B in the discussion of the results) did the departure from the Raman-Nath regime completely preclude the application of δ-function-like kicks to the atoms.

The importance of the phase modulator is due to the dramatic modifications to the dynamics of the kicked atoms wrought by gravity, namely, the quantum accelerator mode [11,28]. It is thus very useful to be able to vary gravity's effect, or even counteract it to such an extent that the behavior of the system is indistinguishable from the case where gravity is truly absent. When the standing wave is shifted in this way so as to remove gravity's effect, the system is, of course, not completely equivalent to one located in a zero-gravity environment because the rest frame of the atoms in our system is not an inertial frame. In general relativistic terms, the rest frame of the atoms in our experiment is not equivalent to the rest frame of atoms in the genuine absence of gravity. However, this distinction has no effect on the dynamics of our experimental system. Hence we do have the capability of investigating how atoms react in a reduced- or zero-gravity environment.

In order to quantify the effect of noise, we use additional laser pulses of controllable intensity. Between each pulse of standing wave light, a 4.5-μs pulse of $D2$ light, red detuned by 60 MHz from the $F=4\rightarrow F''=5$ transition, is applied. This induces, with a laser-intensity-dependent probability, a transition in an atom after which spontaneous emission will occur. The mean number of induced emissions per atom per $D2$ pulse is varied between 0 and 0.2. This technique is similar to that used in Refs. [35,38], in which, however, lower levels of spontaneous emission were generally utilized. On the other hand, in Refs. [39,40], the effect of amplitude noise was investigated, and the noise level was generally significantly higher than that used in our work.

Noise has the effect of randomizing the phase of the wave function of the atom undergoing the transition by introducing a randomly directed change in its momentum of magnitude $\hbar k_2$. This upsets the coherence of the evolution from pulse to pulse and introduces momentum and hence phase-noise into the system. Note that there is always a background rate of spontaneous emission due to the $D1$ light of the standing wave, which is less than 2×10^{-3} per atom per pulse and negligible in its effect on the system's development for the number of pulses that we are applying. There is also amplitude noise in the potential experienced by the atoms due to fluctuations in the power of the $D1$ light forming the standing wave and its detuning. Though small in comparison with the noise applied through spontaneous emission, its effect is not completely negligible and will be discussed both later in this section and in Sec. IV.

The experiments were performed in two different configurations: with and without the counteraction of gravity's effect, constituting the δ-kicked rotor and the δ-kicked accelerator, respectively. After the prescribed number of kicks, the momentum distribution was measured, the results being averaged over three runs. The mean energy of the ensemble of atoms was then determined from the averaged momentum distribution. These energy values are subject to a degree of uncertainty because those atoms in the wings of the momentum distribution, where the signal-to-noise ratio is worst, contribute the most significantly to the mean energy. Thus noise in the signal (''signal noise'') (as opposed to noise introduced by application of $D2$ light) can seriously affect the results. The problem of signal noise in the TOF distribution was most significant in the cases where a large level of spontaneous emission-inducing $D2$ light was applied, thus reducing the size of the signal.

The TOF method measures the population of atoms over a fixed range of momenta: $\pm75\hbar G$. The extent of the experimental momentum distribution of atoms, however, was always less than this range (and never exceeded $\pm60\hbar G$), so it was always necessary to impose a momentum boundary beyond which the data would not be taken into account, as any signal in the extrema must be noise. The value of this momentum boundary depended on the momentum width of the atoms. Additionally, to minimize the effect of the signal noise within the limits specified by the boundary, it was necessary to impose a signal threshold below which data was ignored. Both the boundary and the threshold were chosen so as to cause negligible degradation to the important features of the observed variation in the mean energy, while at the same time reducing the noise present in that variation. For different experimental configurations, different values of the number of pulses applied or of the pulse period led to different momentum widths. The momentum boundary for a given configuration was chosen so that when the atomic momentum distribution was at its widest, as much as possible of it, while as little as possible of the signal noise in the momentum range beyond, was included. This procedure meant that in the case where the atomic momentum distribution extended close to the imposed momentum boundary, the momentum possessed by a very small fraction of atoms in the wings of the distribution was neglected, thus lowering the mean energy below its true value. We estimate the reduction in the measured mean energy of the atoms due to the imposition of a signal threshold, and due to the momentum cut, to be in each case less than 5%. On the other hand, in the case where the atomic momentum distribution was much narrower than the included momentum range, the signal noise with amplitude greater than the threshold and lying within the momentum boundary led to a mean energy background upon which the true mean energy of the narrow atomic momentum distribution was superimposed. Hence the values of mean energy calculated using the experimental data were higher than would be expected due to the atoms alone in the absence of signal noise. In the case of the narrowest momentum distributions, this led to a 5% increase in the calculated

mean energy due to the signal noise; for wider momentum distributions the fractional increase was smaller than this.

The fact that the laser power delivered to the vacuum system to create the standing wave varies by $\sim 10\%$, and the detuning of this $D1$ light varies by $\sim 0.3\%$, means that the depth of the potential experienced by the atoms fluctuates by $\sim 10\%$. This amplitude noise in the potential is another respect in which our experimental system is nonideal and leads to quantitative disagreement between the mean energies as calculated from the experimental data and those which would be expected in a noiseless system. Moreover, in an ideal system all atoms experience the same potential. However, in our system the diameter of the trap is somewhat larger than the waist of the beam of $D1$ light. This means that about 25% of the atoms (those on the periphery of the MOT) experience a potential sufficiently reduced below the maximum value that the potential's effect on their dynamics is small compared with that on atoms in the center of the MOT. Therefore, in the experiments where $D1$ light pulses caused a significant broadening of the momentum distribution, the smaller response of these atoms led to a lower mean energy than would be expected if all atoms were exposed to the same potential. The mean energy of the atomic ensemble was approximately half the value that would be obtained if all the atoms experienced the mean value of $\phi_d = 0.8\pi$ (see discussion in Sec. IV A). This goes a long way towards explaining the quantitative difference in the mean energies calculated from the simulations and the experiment in the case of the δ-kicked accelerator, for which there is considerable broadening of the momentum distribution.

B. Numerical methods

The numerical simulations model idealized quantum and classical versions of our experimental system, and can include the effect of noise. The classical model consists of an iteration of Eqs. (2) and (3), and takes into account the experimental kicking strength and initial distribution of the atoms in position and momentum. In our experiment the atoms are initially distributed almost uniformly over a given period of the potential. Their initial distribution in momentum is Gaussian, centered around zero with a FWHM of $12\hbar k_2$. The simulation propagates 10^5 trajectories with a range of initial conditions that reflects these experimental distributions and gives the momentum distribution of the particle ensemble at any subsequent time. The calculation of the mean energy from this is straightforward.

In the quantum-mechanical case, we first consider the effect of the kicking potential. Using the identity

$$\exp[-i\phi_d \cos(\hat{\chi})] \equiv \sum_{n=-\infty}^{\infty} (-i)^n J_n(\phi_d) \exp(in\hat{\chi}), \quad (6)$$

we see that the effect of a kick can be decomposed into an infinite sum of momentum displacement operators $\exp(in\hat{\chi})$ weighted by nth-order Bessel functions of the first kind, $J_n(\phi_d)$ [we have ignored an irrelevant global phase $\exp(-i\phi_d)$]. When applied to a plane wave $\psi(\chi) \propto \exp(i\kappa\chi)$ this is fully equivalent to the effect of a phase grating. A plane wave in this form with scaled wave number κ corresponds to a momentum eigenstate with eigenvalue $\kappa\hbar G$. For the interkick free-evolution operator, we can factorize the $\hat{\chi}$ and $\hat{\rho}$ dependent parts, resulting in

$$\exp[-i(\gamma\hat{\chi} + \hat{\rho}^2/2)/\tau] \equiv \exp[-i(\hat{\rho}^2 + \gamma\hat{\rho})/2\tau] \times \exp(-i\gamma\hat{\chi}/\tau)\exp(-i\gamma^2/4\tau). \quad (7)$$

It is readily seen that $\exp(-i\gamma\hat{\chi}/\tau)$ is also simply a momentum displacement operator, describing free fall due to gravitational acceleration between pulses, and that $\exp[-i(\hat{\rho}^2 + \gamma\hat{\rho})/2\tau]$, when applied to a momentum eigenstate, will simply provide a phase. We will ignore the global phase $\exp(-i\gamma^2/4\tau)$ from now on. The fact that the Floquet operator can be decomposed into a combination of momentum displacement operators and terms proportional to the momentum operator makes a basis of momentum eigenstates an obvious choice for numerics. This is a direct result of the fact that what is taking place is diffraction of the de Broglie waves. We, in fact, use a basis that is offset by $-\gamma/\tau$ in momentum between successive iterations. This is how we incorporate the effect of $\exp(-i\gamma\hat{\chi}/\tau)$, although the actual momentum must be used when determining the phase ϕ_n accumulated between successive pulses. In vector notation, we thus define $|n\rangle$ to be a basis state with a scaled momentum immediately prior to the Nth pulse given by $\rho_{n,N} = \rho_i + n\tau - (N-1)\gamma$, where ρ_i is the initial scaled momentum of the plane wave in the direction of the applied standing wave. Using this notation we can depict the effect of the kick as

$$\hat{U}^{\text{int}}_{mn} = (-i)^{m-n} J_{m-n}(\phi_d) |m\rangle\langle n|, \quad (8)$$

where m and n are the final and initial diffraction orders, respectively [13]. The free evolution is then expressed by

$$\hat{U}^{\text{free}}_{mn} = \exp(i\phi_n)\,\delta_{mn} |m\rangle\langle n| \quad (9)$$

where

$$\phi_n = \frac{1}{2\tau}[\rho_i^2 + (n\tau)^2 + N(N-1)\gamma^2 - \gamma(2N-1)(\rho_i + n\tau) + 2n\tau\rho_i]. \quad (10)$$

The initial distribution is assumed to be an incoherent superposition of plane waves with different values of their momentum component along the axis of the periodic potential. Each of these is treated separately and the results are added incoherently by summing probabilities. The relative populations of different initial momenta (deduced from the initial experimental momentum distribution) are taken into account in the simulation. The result of the simulation is the probability, for each initial plane wave, of occupation of each possible momentum state up to $\rho = \pm 60\tau$ ($\Rightarrow p = \pm 60\hbar G$), i.e., the probability of having acquired each of these momenta from the kicking potential. This information

allows us to construct the final state momentum distribution of the ensemble and hence find the mean energy.

In the case where spontaneous emission is present, the momentum of the particle (in the classical case) or the value of $\rho_{n,N}$ (in the quantum case) is modified if an atom undergoes spontaneous emission. However, only the momentum component along the axis of the sinusoidal potential is of significance as far as the kicked dynamics are concerned. Since spontaneous emission is a statistical process, a Monte Carlo technique is used such that there is a certain probability per atom per kick (determined by the level of $D2$ light applied to the atoms) of a spontaneous emission taking place. The spontaneously emitted photons are also regarded as being equally likely to be emitted in any direction. To take account of the stochastic nature of the decay process, the quantum simulation in each case is repeated ten times and the average taken, whereas the classical system already includes a sufficient degree of averaging due to the 10^5 trajectories that are simultaneously propagated with the appropriate probability per unit time of a spontaneous emission taking place.

IV. RESULTS

A. Variation in mean energy with pulse number

Following the example of Refs. [10,35], we study the change in the mean energy of the ensemble with kick number, the characteristics of which differ markedly between classical and quantum-mechanical systems and are strongly influenced by the presence of noise. We set $T=60.5\ \mu$s, and consider situations where the applied noise levels are 0 and 0.2 spontaneous emissions per atom per pulse, both including and counteracting gravity. We have chosen T so that, in the zero applied-noise regime, we expect to observe a quantum accelerator mode when the effect of gravity is included (δ-kicked accelerator), and dynamical localization when gravity is counteracted (δ-kicked rotor). Data from experiments, quantum simulations, and classical simulations are displayed in Fig. 2; note that the momenta are measured after having subtracted the offset due to gravitational free fall, and it is from these momenta that the mean energies are calculated. The same momentum boundaries were applied to the quantum simulations as to the data. No boundaries were applied to the classical simulation because localization does not occur, and the cuts would have resulted in part of the wider momentum distributions being neglected (something the data cuts were specifically chosen not to do). This would lead to an entirely spurious fall-off in the rate of increase in mean energy for larger pulse numbers when the distribution is wide. Assuming the downward and retroreflected beams to be exactly counterpropagating and perfectly aligned with the MOT, the standing wave to have a Gaussian profile, and the power in the beams creating the standing wave to be ~ 120 mW, the estimated mean value of ϕ_d is half the estimated maximum value, and is $\sim 0.9\pi$. However, due to the uncertainty in the precise value of the light intensity experienced by the atoms, the diameter of the MOT and the alignment of the beams creating the standing wave, mean values of ϕ_d between 0.5π and 1.5π would not be incompatible with our

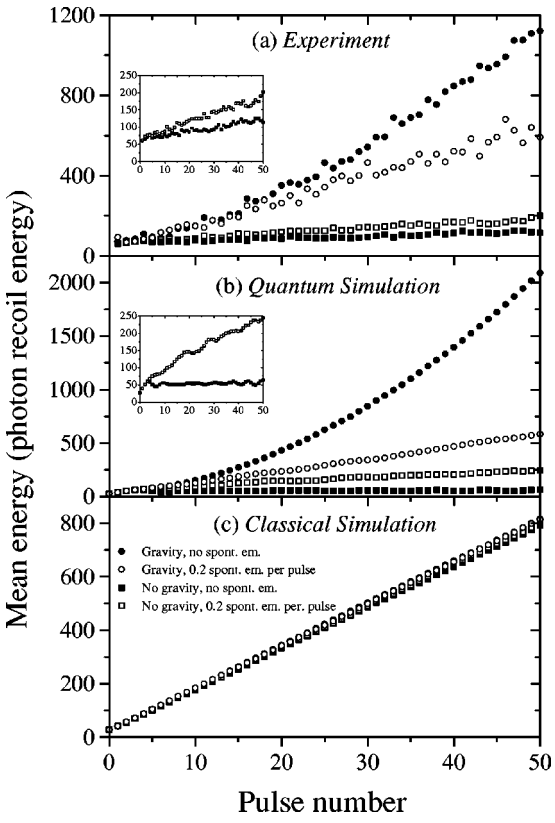

FIG. 2. Variation of mean energy with pulse number with $T=60.5\ \mu$s; (a) experimental results with light detuning of 30 GHz and beam power of ~ 120 mW, (b) quantum simulation with $\phi_d=0.8\pi$, (c) classical simulation with $\phi_d=0.8\pi$. The momentum cuts used for the data and quantum simulation are $\pm 60\hbar G$ for the δ-kicked accelerator and $\pm 30\hbar G$ for the δ-kicked rotor. No cuts are applied to the output of the classical simulation (see text). The inset figures in (a) and (b) show, on an expanded y axis, the variation of the mean energy with pulse number for the δ-kicked rotor, both with and without added spontaneous emission, as calculated using data from the experiment and quantum simulation, respectively. Where induced spontaneous emission is present, the mean number of emissions undergone by an atom per pulse is ~ 0.2. The experimental energies for the δ-kicked accelerator in the absence of induced spontaneous emission are systematically lower than those of the simulation because of the reduced interaction of part of the experimental ensemble of atoms with the potential, imperfect fulfilment of the conditions for being in the Raman-Nath regime, and amplitude noise in the potential. Those for the δ-kicked rotor are systematically higher, in the absence of added noise, due to signal noise in the wings of the momentum distribution and amplitude noise in the potential (see text).

known experimental parameters. Numerically, we take $\phi_d=0.8\pi$, a value which gives closer agreement with the experimental data and is well within the range of experimental uncertainty in the value of ϕ_d. This means that $I_{\max}=0.8\pi\hbar G$. The equivalent classical regime is not one where we expect to see significant anomalous diffusion due to classical accelerator modes.

In Figs. 2(a) and 2(b), we observe good, though not perfect, qualitative agreement between the experimental and nu-

merical quantum systems. Note that, as stated in Sec. III A, in the experimental system we effectively have a range of different values for ϕ_d, depending on the positions of the individual atoms in relation to the beam profile, rather than each atom being kicked with equal strength. As the exact fraction of atoms experiencing a given value of ϕ_d is unknown, it is impractical to take this variation fully into account numerically. In any case, the simulations are used so as to highlight the features of the physical behavior, and this is better achieved by using a unique value of ϕ_d. The value of $\phi_d = 0.8\pi$ should be understood as an approximate mean value, which should yield qualitatively correct dynamics, not precise quantitative agreement. The quantitative agreement is also impaired due to the effect of momentum boundaries and signal threshold that were discussed at the end of Sec. III A, and due to the fact that there is always some noise present in the experimental system.

The qualitative agreement we observe nevertheless confirms our theoretical understanding of the experimental system, particularly the prediction of strikingly different behaviors due to quantum-mechanical effects in the zero applied-noise case. For the δ-kicked accelerator, the mean energy increases much faster than linearly, almost quadratically, with pulse number, due to the presence of a quantum accelerator mode, which dominates the mean energy of the ensemble. It is evident that after ~ 25 pulses, the experimentally measured energy growth is not as rapid as for the quantum simulations, and is in fact approximately linear. This is because as the atoms accelerate they increasingly leave the Raman-Nath regime. The momentum attained by the accelerated atoms after 50 pulses in this experimental configuration ($T = 60.5$ μs), due to both kicks and gravitational acceleration, is $\sim 57\hbar G$, meaning that atoms move through 0.38 standing wave periods over the duration of the pulse. This causes an effective reduction in the value of ϕ_d, leading to reduced diffraction efficiency, and hence population in the accelerator mode, with increasing pulse number. In the simulations we apply perfect δ-kicks, hence we are by definition always in the Raman-Nath regime. Additionally, the amplitude noise in the potential depth (up to $\sim 10\%$ variation) caused by fluctuations in the power in the standing wave and the detuning of the $D1$ light reduces the efficiency of population of the accelerator mode. This noise is not present in the idealized situation modeled in the simulation, so is also a source of quantitative disagreement.

When the effect of gravity is counteracted (δ-kicked rotor), the mean energy of the system shows a much reduced rate of increase beyond a certain pulse number, corresponding to the quantum break time (the third or fourth pulse, in our case), and displays small-amplitude quasiperiodic oscillations. These effects can be seen in the inset figures in Fig. 2 and are particularly clear in (b), which shows the data from the quantum simulation. The evident difference between the behavior in the experiment and in the quantum simulation is due to the fact that the experiment is not a noiseless system, even when we do not induce additional spontaneous emission through applied $D2$ light, due to the variation in the depth of the periodic potential. This amplitude noise causes some disruption to the process of dynamical localization,

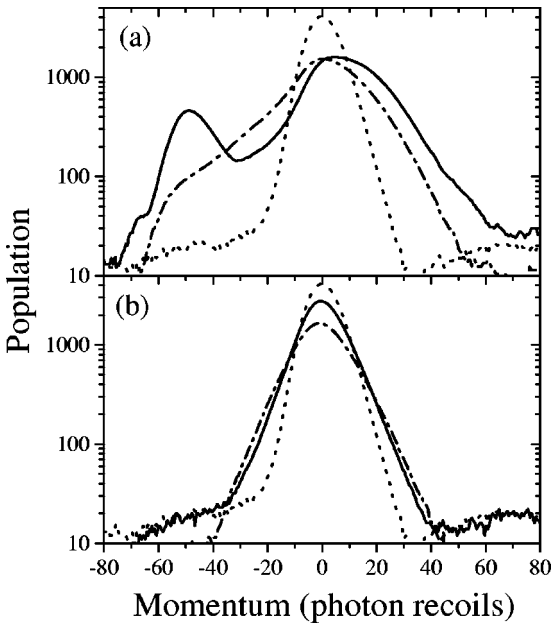

FIG. 3. Experimentally measured momentum distributions, showing the initial distribution of the momenta of atoms in the MOT (dotted line), the distribution after 30 pulses at $T = 60.5$ μs without applied noise (solid line) and the distribution after 30 pulses at $T = 60.5$ μs with applied noise of 0.2 spontaneous emissions per atom per pulse (dash-dotted line). In (a) gravity's effect is present, and this is example of a quantum accelerator mode in the δ-kicked accelerator. In (b) gravity's effect is compensated for; this is an example of dynamical localization in the δ-kicked rotor.

leading to nonzero quantum diffusion after the quantum break time. However it is much less than that which results from the disruption to the evolution caused by spontaneous emission (described below) so that the suppression of the momentum diffusion rate after the quantum break time has been exceeded is still observable. The effect of this level of amplitude noise is consistent with that observed in Refs. [39,40]. The quasiperiodic oscillations are more difficult to discern unambiguously in the data, though the data are not inconsistent with the result of the simulation. Simulations using different values of ϕ_d show that the period of these oscillations depends on ϕ_d and, in fact, decreases as ϕ_d increases. The fact that the trapped atoms experience a range of laser intensities means that the resultant variation of the mean energy of the ensemble with pulse number is a superposition of oscillations with different periods. This tends to wash out the quasiperiodic oscillations in the data, whereas they are clearly visible in the simulations performed with a unique value of ϕ_d. Nonresonant quasiperiodic oscillatory behavior of the type present here has been observed in numerical simulations of the quantum δ-kicked rotor [32,49,50]. The cessation of energy growth is due to dynamical localization, where the momentum distribution is exponential in form and does not broaden further after the quantum break time. Figure 3 shows experimentally measured momentum distributions after 0 and 30 pulses for both gravitational scenarios in the presence and absence of applied noise. The apparent asymmetry in the extreme wings of each

distribution is, as explained in Sec. III A, due to the lock-in amplifier that was used to amplify the signal from the TOF measurement. The size of the signal in the region where this asymmetry is evident is so small that it is below the level of the signal threshold imposed on the data and therefore does not enter the calculations of the mean energy.

That the differences in observed behavior between the cases where gravity's effect is unaltered (δ-kicked accelerator) and where it is counteracted (δ-kicked rotor) are intrinsically quantum mechanical is made particularly obvious by the classical simulations plotted in Fig. 2(c), where, in contrast to Figs. 2(a) and 2(b), the difference in energy growth for each case is only just noticeable. In each case the mean energy increases essentially linearly with pulse number, i.e., $\alpha=1$ in Eq. (5). We are not in a regime of anomalous diffusion, and the particles effectively execute random walks in momentum space. This behavior is evidently quite different from that of the observed quantum-mechanical case in the zero applied-noise regime.

Upon the addition of noise via spontaneous emission, the behavior of our quantum-mechanical system is affected dramatically. Firstly, the pronounced quantum-mechanical effects of enhancement or inhibition of momentum diffusion have been diminished. This is also clear from Fig. 3. For the δ-kicked accelerator, the effect of the noise has been to greatly reduce the population of the accelerator mode, while for the effective δ-kicked rotor the distribution is still apparently exponential, but has broadened such that its FWHM has increased by $\sim 30\%$. This is consistent with the observations reported in Refs. [37,38]. Secondly, the behavior is less dependent on the presence or absence of gravity, i.e., the cases of the δ-kicked accelerator and the δ-kicked rotor are less distinct from one another, in that the pronounced asymmetry in the δ-kicked accelerator distribution has been almost removed, the difference in the widths of the distributions has been reduced and in both cases the distribution continues to broaden with increasing pulse number. Thirdly, the behavior in the two cases is similar to that of the theoretical classical system in Fig. 2(c) in terms of the linear variation in mean energy with pulse number. We can immediately say that we have made the behavior of the system more classical *in appearance* by the introduction of noise because the responses of the two systems to the application of the kicks, as expressed by mean energy growth, are more similar to one another. By randomizing the phase of the wave packet due to the momentum impulse imparted by spontaneous emission, we have prevented the diffracted momentum orders from achieving the correct phase relationship at the time of the next pulse. For the δ-kicked accelerator this means that constructive interference of progressively higher diffracted orders to yield a linear increase in the momentum of a fraction of the atoms does not occur. For the δ-kicked rotor, the destructive interference leading to dynamical localization is similarly absent. Thus diffusion continues even after the quantum break time has been exceeded; this is the quantum diffusion referred to in Sec. II. The system cannot be said to be classical, but, because some of its behavior, viz., the linear rise of mean energy with pulse number, can be described by a classical model, it is in this sense ''classical-like.''

For the classical system of Fig. 2(c), the effect of spontaneous emission is small, resulting in a very small decrease in the mean energy attained after a given number of pulses when gravity's effect is present, and a slightly larger increase when gravity's effect is absent. This is because, in the absence of noise, there is a degree of kick-to-kick correlation for some particle trajectories, which, for this value of T, promotes momentum transfer to these particles when gravity is present and inhibits it when gravity is absent (this will be addressed in more detail in Sec. IV B). The effect of random momentum kicks resulting from spontaneous emission is to destroy these correlations, and hence the diffusion rate is slightly altered as stated.

In the case shown in Fig. 2(c), $\alpha=1$ for all the classical systems shown, with or without noise and/or gravity, and we observe a linear mean energy increase in the noise-perturbed quantum system. Thus the quantum system behaves more like the classical. If we were applying a level of noise such that it dominated the energy growth of the classical system, this result would not be surprising since the effect of the noise would be expected to swamp all others in the quantum system as well [30]. However, since we are operating in a regime where the effect of noise on the classical system is small, its marked effect on the quantum system [51], resulting in a convergence in the behavior of the two cases, is important. Such convergence of quantum and classical behavior in the δ-kicked rotor system has previously been observed in the work reported in Refs. [35,36,38–40]. The effect of the levels of spontaneous emission used in our experiment on the mean energy attained after 50 pulses in the case where gravity's effect is counteracted is consistent with that shown in Refs. [35,36] by Ammann *et al.* and Ref. [38] by Klappauf *et al.* The noise used in Refs. [39,40] was amplitude noise, and generally of a much higher level than the noise in our experiment, though the conclusions reached are also consistent with our assessment of the behavior of the system.

B. Variation in mean energy with pulse period

Another useful approach when considering the behavior of the mean energy is to determine its variation with changing values of different experimental parameters for a set number of pulses. There are three basic parameters that determine the dynamical behavior of the system: K, γ, and the quantum-mechanical τ. These can all, in principle, be varied independently by changing $I_{\max}$, G, T, or the effective value of g. However, due to the geometry of our system, it is inconvenient to vary G by creation of the standing wave potential using counterpropagating laser beams where the angle between them is not equal to π. The intensity, and hence $I_{\max}$, can be varied, though with much less precision than is possible for g and T. Experimentally, therefore, we either left gravity's effect unaltered (δ-kicked accelerator), or counteracted it as completely as possible using the phase modulator (δ-kicked rotor), and in both cases varied T be-

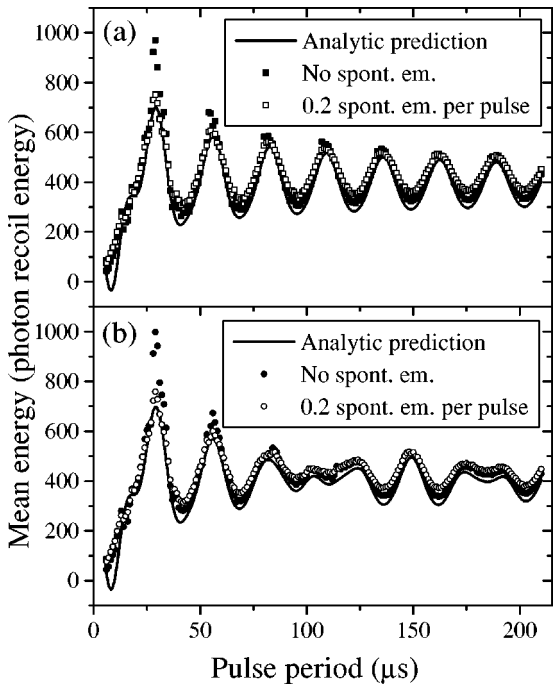

FIG. 4. Variation of mean energy with pulse period according to classical simulation and the analytical prediction of Eq. (11) for 30 pulses with $\phi_d = 0.8\pi$, (a) in the absence of gravity (δ-kicked rotor), (b) in the presence of gravity (δ-kicked accelerator). No momentum cuts have been applied to the results of the simulation. Where it is nonzero, the mean number of spontaneous emissions undergone by an atom per pulse is 0.2.

tween 6.5 μs and 210.5 μs in steps of 1 μs. The set number of pulses used was 30, and $I_{\max}$ was held constant.

In the classical case the global level of momentum diffusion in the system is well described by the diffusion parameter $D(K,\gamma)$, where

$$D(K,\gamma) = \frac{K^2}{2}\left[\frac{1}{2} - J_2(K)\cos(\gamma) - J_1^2(K) \times \cos(2\gamma) + J_2^2(K) + J_3^2(K)\right], \qquad (11)$$

and $J_n(K)$ is the nth-order Bessel function of the first kind. It follows that the mean energy is given by $\overline{E_N} = NmD(K,\gamma)/(GT)^2$, where, as before, this is determined after having subtracted from the momenta the offset due to gravitational free fall. The expression for $D(K,\gamma)$ can be determined using the method of Fourier paths [12] (see the Appendix for an outlined derivation). This expression includes the effect of low-order kick-to-kick correlations [hence the presence of the Bessel function corrections to the random phase result $D(K) = K^2/4$], although, since it always assumes linear diffusion, it cannot fully incorporate the effect of highly correlated classical accelerator modes. Obviously, if $\gamma = 0$ we regain the usual δ-kicked rotor result [12].

Figure 4 shows the variation, when 30 kicks are applied in both the presence and absence of gravity's effect (δ-kicked accelerator and δ-kicked rotor, respectively), in the mean energy of the classical system where $\phi_d = 0.8\pi$ and T is varied (thus K varies linearly between 1.2 and 49.7). This variation is calculated from the analytical prediction given by Eq. (11), and from numerical simulations, both with and without noise. Note that the numerical simulations assumed a Gaussian initial momentum distribution (the initial position distribution is uniform), corresponding to the experimental situation, whereas the prediction of Eq. (11) assumes a uniform distribution in both position and momentum. This may slightly skew the numerical result relative to the analytical prediction. Note, however, that even if an initially uniform distribution is employed for the numerics then, in spite of generally excellent qualitative agreement, quantitative agreement is not perfect [12].

The size of the peaks in mean energy as shown in Fig. 4 is enhanced relative to the analytical prediction of the value of $D(K,\gamma)$ by the occurrence at these kicking intervals of superdiffusive energy growth: a fraction of the atoms fulfil the criteria for entering a long-lived classical accelerator mode [12] due to momentum growth-enhancing correlations. On the other hand energy growth at the troughs is subdiffusive, as there are momentum diffusion-inhibiting correlations. At these extremes the analytical prediction is imperfect due to its failure to take into account all correlations.

The effect of gravity on the behavior of the system is clear from comparison of Figs. 4(a) and 4(b). For small values of the pulse period, gravity has little effect [γ is small and therefore the γ-dependent cosines in $D(K,\gamma)$ have negligible effect]. However, for larger values the additional change in position and momentum due to gravitational acceleration is increased. This will obviously change the initial conditions that lead to normal and anomalous diffusion for different values of T. In the presence of gravity (δ-kicked accelerator), the accelerator modes that do occur can only exist in one or the other direction in momentum space, never both simultaneously, as in the zero-gravity (δ-kicked rotor) case. This is because gravity has broken the symmetry of the system.

The effect of adding a spontaneous emission rate of 0.2 per atom per pulse does not dramatically alter the dynamics either in the presence or absence of gravity. This was referred to in Sec. II and is discussed in Ref. [29]. As the peaks and troughs observed in the variation of the mean energy are due to kick-to-kick correlations, and as the addition of noise disturbs these correlations, the observed effect is a general flattening of these oscillations as the probability of spontaneous emission rises. This can be seen in Fig. 4, and is consistent with the classical numerical data plotted in Fig. 2(c).

The experimental results, plus those of the quantum simulations, for the δ-kicked accelerator are shown in Fig. 5, where again the mean number of spontaneous emissions per atom per period due to the applied $D2$ light was either 0 or 0.2. The corresponding results for the configuration in which gravity was compensated for (δ-kicked rotor) are shown in Fig. 6. When comparing our experiments with quantum simulations, we again see good qualitative agreement. The same experimental imperfections addressed in Sec. IV A apply equally here, and are responsible for quantitative discrep-

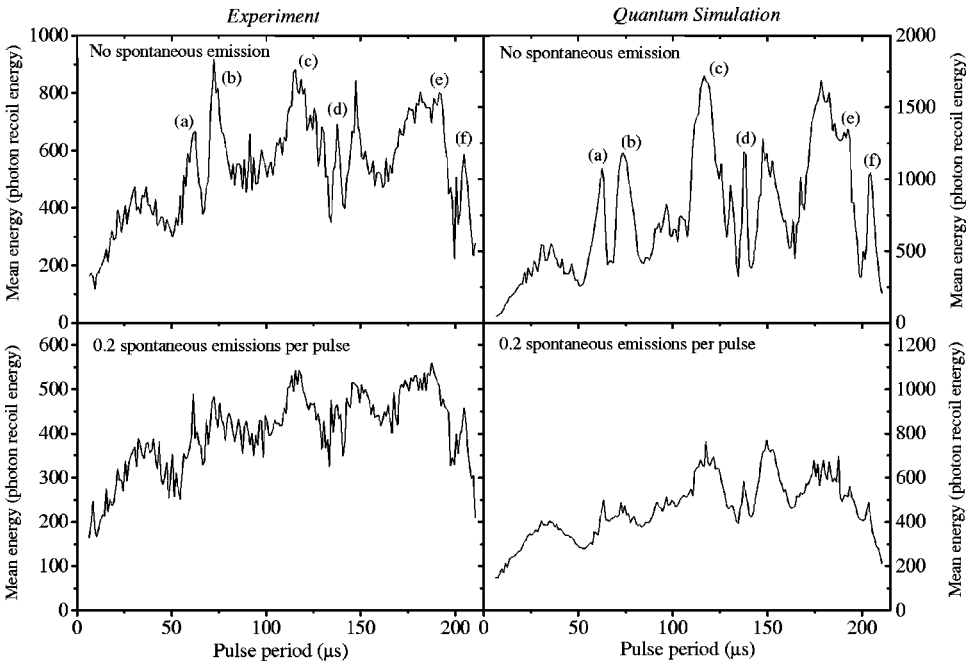

FIG. 5. Variation of mean energy with pulse period after 30 pulses when gravity's effect is not counteracted (δ-kicked accelerator). The momentum cut used is $\pm 60\hbar G$. Where induced spontaneous emission is present, the mean number of emissions occurring per atom per pulse is ~ 0.2. Experimental results are for a light detuning of 30 GHz and beam power of ~ 120 mW. Quantum simulation results are for $\phi_d = 0.8\pi$. The labels in the top two panels are discussed in the text. Note that the vertical scales in the simulation graphs differ by a factor of 2 from those of the corresponding experimental graphs.

ancies. As before, the same momentum cuts were applied to the simulation results as to the experimental data. There is a clear offset to the experimental mean energies; this is because of background noise in the wings of the measured momentum distributions, as discussed in Sec. IV A, and the broadening of the atomic momentum distribution due to amplitude noise in the potential.

The behavior in the quantum-mechanical system is very

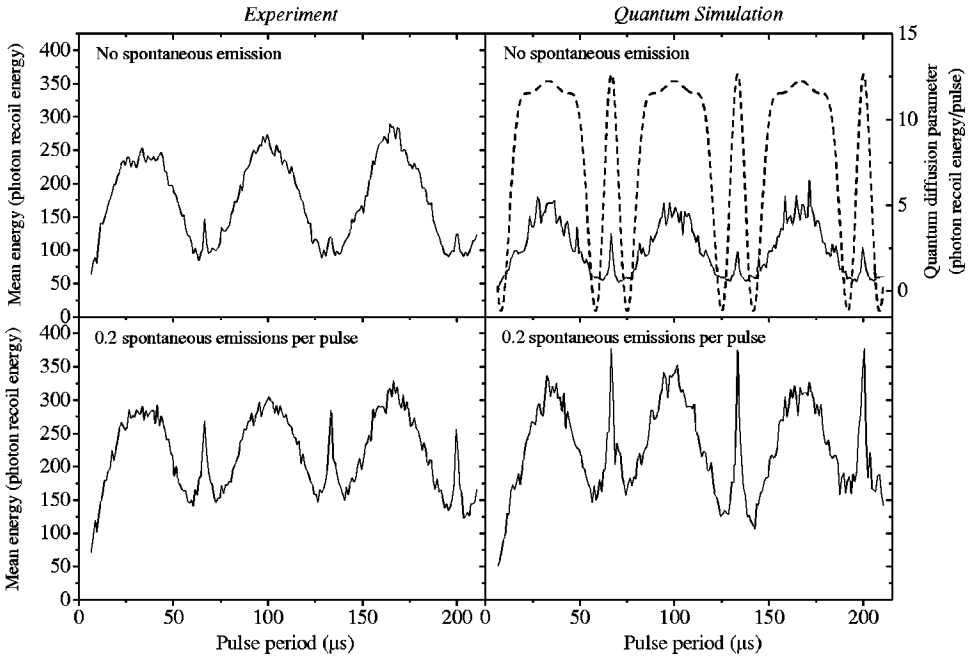

FIG. 6. Variation of mean energy with pulse period after 30 pulses when gravity's effect is counteracted (δ-kicked rotor). The momentum cut used is $\pm 40\hbar G$. Where induced spontaneous emission is present, the mean number of emissions occurring per atom per pulse is ~ 0.2. Experimental results are for a light detuning of 30 GHz and beam power of ~ 120 mW. Quantum simulation results are for $\phi_d = 0.8\pi$. Note that the vertical energy scales in all the graphs are the same. The variation of the initial value (i.e., at the first pulse) of the quantum diffusion parameter $D(K_q)$ (see text) when $\phi_d = 0.8\pi$ has been plotted as a dashed line over the values of the mean energy of the δ-kicked rotor system calculated from the quantum simulation. This shows that the maxima and minima of the analytical parameter expressing the extent of the momentum diffusion coincide with the observed maxima and minima of the mean energy. The negative values of this quantity are not physical and result from the fact that the expression for $D(K)$ in Eq. (11), which is used to obtain $D(K_q)$, is a truncated series. Inclusion of higher-order terms would avoid this unphysical result, but would not change the gross features of the variation with pulse period.

different from that of the classical system, and is strongly dependent on both the effect of gravity and the level of spontaneous emission. The most important difference between the two cases (δ-kicked rotor and δ-kicked accelerator) with zero-induced spontaneous emission is the existence of the pronounced peaks (a) and (b) in the mean energy to either side of $T=66$ μs for the δ-kicked accelerator (see Fig. 5). These peaks indicate quantum accelerator modes. The peaks (c), (d), (e), and (f) are also due to gravity-induced accelerator modes. All the labeled peaks correspond to a lower value of the mean energy in the experiment than in the simulation. As described in Sec. IV A, amplitude noise in the potential and the leaving of the Raman-Nath regime with increasing atomic momentum reduce the efficiency of population of the accelerator mode, so these lower experimental values are expected. Peaks (c) and (e) are smaller (relative to the surrounding energies) in the experimental data than in the simulation. In this experimental configuration (30 pulses applied, $T=115.5$ μs, 191.5 μs, respectively) the momentum of the fastest-moving atoms relative to the standing wave, when the effect of gravity is taken into account, is greater than $72\hbar G$ (higher than the $57\hbar G$ attained after 50 pulses with $T=60.5$ μs). When the atoms have attained momenta in this region, they have left the Raman-Nath regime because they move through a significant fraction (>0.5) of the period of the standing wave over the duration of an individual pulse. This means that they cannot experimentally be accelerated up to these momenta or further with great efficiency. Thus the experimental population of such high-momentum states is low. The simulation, however, assumes kicks that are truly δ functions so that the atoms are always in the Raman-Nath regime and can be accelerated efficiently to arbitrarily high momenta. Thus the peaks here are larger in the simulation than in the experiment.

When the effect of gravity is counteracted (δ-kicked rotor), the momentum distribution is exponential in form [as shown in Fig. 3(b)] after 30 pulses for all pulse periods studied except $T=66.5$ μs, $T=133.5$ μs, and $T=200.5$ μs. For pulse periods other than these, dynamical localization is setting or has set in. The localization length varies as T varies, thus explaining the observed variation in the mean energy, as shown in Fig. 6. The proportionality of the quantum break time to the localization length, and their variation with the quantum version of the classical diffusion parameter $D(K)$ [12] are explained in Refs. [32,52]. The values of the localization length and quantum break time are proportional to the quantum diffusion parameter $D(K_q)$, i.e., the quantity obtained when $K_q=2K\sin(\pi/2)/\tau$ is used in the expression for the classical diffusion parameter $D(K)$ (as employed, for example, by Klappauf *et al.* [44]). The quantity $D(K_q)$, whose value is expressed here in units of energy per pulse, has been plotted on Fig. 6 over the variation of the mean energy as calculated from the quantum simulation for the δ-kicked rotor. $D(K_q)$ in these units gives the initial rate of increase in the mean energy with pulse number. At higher pulse numbers, however, the energy value obtained by multiplying $D(K_q)$ by the pulse number will not give the correct mean energy of an ensemble of atoms. This is because as dynamical localization begins to occur (and the smaller the quantum break time, the earlier this happens), the effective diffusion parameter decreases [53], eventually falling to zero. The initial value of $D(K_q)$ is a good indicator of the extent of energy transfer to the system, and it is clear that the maxima and minima in $D(K_q)$ and in the mean energy are coincident, including the quantum resonance spikes at $T=66.5$ μs, $T=133.5$ μs, and $T=200.5$ μs (see below). Contrasting the behavior for two different values of T, at $T=30.5$ μs the distribution has not yet localized after 30 pulses (though it has become exponential in form) and continues to broaden with increasing pulse number. On the other hand, at $T=60.5$ μs localization occurs after ~ 3 pulses, after which essentially no further mean energy growth occurs, as shown in Fig. 2 and discussed in Sec. IV A. From Fig. 6, the variation in the mean energy attained after 30 pulses appears periodic when gravity is absent; the period is the half-Talbot time. This periodic variation of the quantum break time and localization length is in agreement with the behavior deduced from $D(K_q)$.

The behavior of the system when $T=66.5$ μs, $T=133.5$ μs, and $T=200.5$ μs merits further discussion. At these times the kicking interval is such that the system is in a quantum resonance. The principal quantum resonance for our system occurs for a pulse period of 133.4 μs (the so-called ''Talbot time'') [11]. Using the notation defined in Sec. II, $\tau=4\pi$ at the Talbot time. The Talbot time is defined using the phase evolved between pulses by diffracted orders from a plane wave that has no initial momentum in the direction of the grating. The Talbot time is the interval between pulses over which adjacent diffracted orders from such a plane wave, in the absence of gravity, accumulate a phase difference through their free evolution of 2π. It is given by $T_{\mathrm{Talbot}}=4\pi m/(\hbar G^2)$. As noted in Sec. II, additional resonances occur for rational multiples of this time. The resonances at 66.7 μs and 200.1 μs are the lowest and second-lowest second-order resonances. Quantum resonances have been investigated experimentally for the δ-kicked rotor [43,44], which has been found to be characterized in these circumstances by a momentum distribution that is nonexponential. Figure 7 shows the momentum distribution of atoms from our MOT after 30 pulses have been applied with $T=66.5$ μs. The significant population in the wings of the distribution, which should be contrasted with that of Fig. 3(b), demonstrates that ballistic acceleration of certain momentum classes of atoms has occurred and confirms that we have a quantum resonance. Both the experiment and simulation indicate that the energy (see Fig. 6) acquired by the system is small for times in the regions around 66 μs, 133 μs, and 200 μs but that the energy acquired by the system when $T=66.7$ μs, 133.4 μs, and 200.1 μs is a local maximum, with a momentum distribution that is nonexponential.

At a quantum resonance there is symmetric, linear growth in the momentum width with pulse number for certain discrete initial values of the quasimomenta. For a system with a continuous initial spread in quasimomenta, as we have, there is a *linear* growth in the mean energy with pulse number in the long-time limit, as explained in Sec. II. For higher-order resonances, this takes a larger number of pulses to manifest

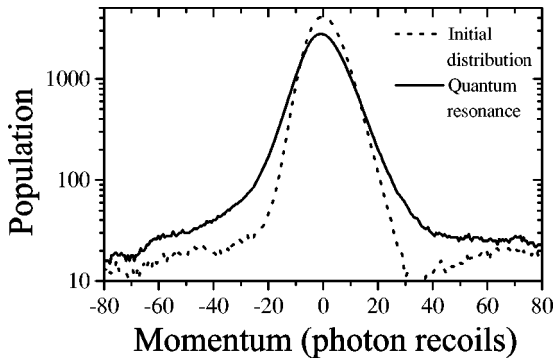

FIG. 7. Experimentally measured momentum distributions, showing the initial distribution of the momenta of atoms in the MOT and the nonexponential form of the distribution after 30 pulses with $T=66.5$ μs when gravity's effect is absent (δ-kicked rotor). This is an example of a quantum resonance, in which ballistic acceleration of atoms in certain momentum classes occurs.

itself, and the resonance itself is narrower in T space than for low-order resonances. The behavior we observe regarding quantum resonances is in agreement with the observations in Ref. [43]; we, however, choose to identify resonances by studying the variation of the mean energy of the system, rather than observation of the form of the momentum distribution itself [43]. The height of the peaks in the mean energy due to quantum resonances, as shown in Fig. 6, is smaller in the experimental data than in the quantum simulation. This is because the experimental population of the high-momentum states causing these peaks in the mean energy is lower than in the simulation due to the imperfect experimental fulfilment by high-momentum atoms of the conditions for being in the Raman-Nath regime.

Additional data (not shown here) show that when ϕ_d is increased, the period between maxima in the mean energy is reduced, although the features in the region of the quantum resonances, and the periodicity determined by the half-Talbot time, remain fixed. Again, this is predicted by the use of K_q in the expression for the diffusion parameter. In the classical system, an increase in ϕ_d results in a similar reduction in the period between maxima in the mean energy.

Turning now to the process of spontaneous emission, with reference to Fig. 5, the most marked effect of its introduction in the presence of gravity is to reduce the height of the pronounced peaks in the mean energy due to the quantum accelerator modes. Since quantum accelerator modes rely for their existence on the correct accumulation of phase by the various diffracted momentum orders, the disruption to this phase due to the spontaneous emission destroys the mode. When the spontaneous emission probability is low (<0.01 spontaneous emissions per atom per pulse) a significant fraction of the atoms will not undergo spontaneous emission during 30 kicks. As the probability grows, the effect of spontaneous emission becomes more serious with the result that the accelerator mode peaks have been greatly degraded when the mean number of spontaneous emissions per atom per kick is 0.2. In fact, the noise reduces the mean energy attained by the system after 30 pulses for all pulse periods; it is just that the destruction of the accelerator mode is the most dramatic effect. When the spontaneous emission level is high, the variation in mean energy with pulse period is rather featureless, due to the destruction by noise of the correlations responsible for accelerator modes. Thus the distinctively quantum effect constituted by the accelerator modes has been degraded by the presence of noise.

For the δ-kicked rotor, see Fig. 6, increasing levels of spontaneous emission increase the mean energy because, on account of the perturbing effect of noise, dynamical localization no longer occurs. The increase in energy is most significant for those values of T where the quantum break time, and hence the mean energy, would be smallest in the absence of noise. The difference in the mean energies of the system in the cases of no applied spontaneous emission and 0.2 spontaneous emissions per pulse is greater in the quantum simulation than in the experiment. This is because, as described previously, the experimental system is not free from the perturbing effects of noise even when no spontaneous emission is induced by applied $D2$ light. Thus in the experiment, dynamical localization has already been degraded to a certain extent without any applied $D2$ light. This means that the mean energies calculated from the experimental data are higher in the ''no spontaneous emission'' case than those calculated from the output of the quantum simulation. The presence of this amplitude noise in the potential also means that when additional noise is introduced by the $D2$ light, the effect is less dramatic in the experiment than in the simulation, where we truly move from a noiseless situation to one in which noise is significant. In the experiment too, noise is significant when the $D2$ light is applied, but it is not negligible when no $D2$ light is applied. Therefore the difference between the behavior in the two situations is not as pronounced as in the simulation.

A very interesting point to note is that, for the δ-kicked rotor configuration, the noise has the effect of degrading the quantum effect of dynamical localization, but of *enhancing* the local maximum in mean energy at the quantum resonances (see Fig. 6). The height of the local maxima at $T\sim 66,133,200$ μs, is increased relative to the energy attained at neighboring values of T, and the width of these peaks is also increased. Since the resonances are a quantum phenomenon, one would have expected noise to remove their signature (the local maxima in energy). This is actually not the case, an observation that is somewhat surprising [53,54].

V. CONCLUSION

We have presented experimental and theoretical results of investigations into the behavior of an atom optical system in which approximate δ-kicks are applied, using a pulsed standing wave of laser light, to cold atoms falling freely under gravity. The effect of gravity can be effectively counteracted by appropriate shifting of the position of the standing wave. The presence of a gravitational potential (δ-kicked accelerator) leads to the occurrence of a specifically quantum-mechanical phenomenon, which we call quantum accelerator modes [11]. When gravity is counteracted (δ-kicked rotor) we observe the well-known effect of dynamical localization

[24]. The effect on the system of the presence of noise has been observed and discussed. The behavior of the system is found to be well described by quantum-mechanical simulations that rely on a diffractive picture of the effect of the periodic potential. Both the experimental results and the quantum simulations indicate that the introduction of noise to the system causes significant degradation to characteristically quantum aspects of the system's behavior, i.e., quantum accelerator modes and dynamical localization. The noise reduces the difference in behavior between the two gravitational scenarios, and results in the restoration of some aspects of the behavior seen in classical simulations, for which the modification in behavior due to the noise is small. The disruption to the coherent evolution of the system by noise, which is formally analogous to the process of continuous measurement [51], makes the quantum dynamics more classical-like, although not identical to the behavior of the equivalent ideal classical system. In this case our system is a noise-perturbed quantum system that exhibits certain characteristics of an ideal classical system.

ACKNOWLEDGMENTS

We thank Professor G. Casati and Professor I. Guarneri of the University of Insubria at Como for stimulating and fruitful discussions, and Dr. M. J. Davis of Oxford University for help in simulation development. This work was supported by the UK EPSRC, the Paul Instrument Fund of The Royal Society, the EU as part of the TMR ''Coherent Matter Wave Interactions'' network Contract No. EBR FMRX-CT96-0002, the European Science Foundation through the BEC2000+ program, and the Alexander von Humboldt foundation.

APPENDIX: DERIVATION OF $D(K,\gamma)$

We have essentially followed the derivation for the δ-kicked rotor diffusion parameter of Chap. 5 of Lichtenberg and Lieberman [12], using the method of Fourier paths and making appropriate modifications to incorporate the effect of γ. Thus the recursion relation for the Fourier coefficients takes the form

$$\begin{aligned} a_n(m,q) = \frac{1}{(2\pi)^2}\int d\chi d\rho \exp[-i(m\chi+q\rho)] \\ \times \int d\chi' d\rho' \,\delta(\rho-\rho'-K\sin\chi'+\gamma) \\ \times \delta(\chi-\chi'-\rho'-K\sin\chi'+\gamma/2) \\ \times \int dq' \sum_{m'} \exp[i(m'\chi'+q'\rho')] a_{n-1}(m',q'), \end{aligned} \tag{A1}$$

which, after integration, becomes

$$\begin{aligned} a_n(m,q) = \sum_{l=-\infty}^{\infty} J_l(|q+m|K) a_{n-1}[m+l\,\mathrm{sgn}(q+m), \\ q+m] \exp[i(q+m/2)\gamma]. \end{aligned} \tag{A2}$$

Through repeated substitution of this recursion relation we arrive at

$$\begin{aligned} a_n(m_n,q_n) = \sum_{l_n,\cdots,l_1} J_{l_n}(|q_{n-1}|K)\cdots J_{l_1}(|q_0|K) a_0(m_0,q_0) \\ \times \exp\left[i\gamma\left(\sum_{k=1}^{n} q_{n-k} - \frac{m_{n-k}}{2} \right) \right]. \end{aligned} \tag{A3}$$

In the case of a path of n steps remaining at the origin in Fourier space, this simplifies to

$$a_n(0,q) = [J_0(Kq)]^n a_0(m_0,q) \exp\left[i\gamma \sum_{l=1}^{n} q\left(q_{n-l} - \frac{m_{n-l}}{2} \right) \right]. \tag{A4}$$

Including the standard low-order corrections by consideration of paths that briefly leave the origin, we determine the following K- and γ-dependent diffusion parameter:

$$\begin{aligned} \tilde{D}_n(K,\gamma) = \frac{K^2}{2}\left[\frac{1}{2} - J_2(K)\cos(\gamma) - J_1^2\cos(2\gamma) \right. \\ \left. + J_3^2(K) + J_2^2(K) \right] - \gamma\overline{\rho_i} + \frac{n\gamma^2}{2}, \end{aligned} \tag{A5}$$

where $\overline{\rho_i}$ is the mean initial scaled momentum. We subtract away the offset due to uniform gravitational acceleration to arrive at the formula we use in Eq. (11) in the text, i.e., $D(K,\gamma) = \tilde{D}_n(K,\gamma) + \gamma\overline{\rho_i} - n\gamma^2/2$.

[1] M.C. Gutzwiller, *Chaos in Classical and Quantum Mechanics* (Springer-Verlag, New York, 1990).
[2] A. Peres, *Quantum Theory: Concepts and Methods* (Kluwer Academic, Dordrecht, 1993).
[3] N. Bohr, Philos. Mag. **26**, 476 (1913); **26**, 875 (1913).
[4] A. Sommerfeld, Ann. Phys. (Leipzig) **51**, 125 (1916).
[5] A. Einstein, Verh. Dtsch. Phys. Ges. **19**, 82 (1917).
[6] L. Brillouin, J. Phys. Radium **7**, 353 (1926).
[7] J.B. Keller, Ann. Phys. (N.Y.) **4**, 180 (1958).
[8] M.S. Child, *Semiclassical Mechanics with Molecular Applications* (Clarendon Press, Oxford, 1991).
[9] This is due to the absence of invariant tori in the classical phase space of nonintegrable systems, as first pointed out by A. Einstein in Ref. [5]. For an extended discussion on this topic, see Ref. [1].
[10] F.L. Moore, J.C. Robinson, C.F. Bharucha, B. Sundaram, and

M.G. Raizen, Phys. Rev. Lett. **75**, 4598 (1995).
[11] M.K. Oberthaler, R.M. Godun, M.B. d'Arcy, G.S. Summy, and K. Burnett, Phys. Rev. Lett. **83**, 4447 (1999).
[12] A.J. Lichtenberg and M.A. Lieberman, *Regular and Chaotic Dynamics* (Springer-Verlag, New York, 1992).
[13] L.E. Reichl, *The Transition to Chaos* (Springer-Verlag, New York, 1992).
[14] G.P. Berman, V.Yu. Rubaev, and G.M. Zaslavsky, Nonlinearity **4**, 543 (1991).
[15] F. Haake, M. Kus, and R. Scharf, Z. Phys. B: Condens. Matter **65**, 381 (1987).
[16] G. Casati, B.V. Chirikov, F.M. Izraelev, and J. Ford, *Stochastic Behavior in Classical and Quantum Hamiltonian Systems* (Springer-Verlag, New York, 1979), p. 334.
[17] M. Stefancich, P. Allegrini, L. Bonci, P. Grigolini, and B.J. West, Phys. Rev. E **57**, 6625 (1998).
[18] N.W. Ashcroft and N.D. Mermin, *Solid State Physics* (Saunders, Orlando, 1976).
[19] S.R. Elliott, *The Physics and Chemistry of Solids* (Wiley, Chichester, 2000).
[20] S. Fishman, D.R. Grempel, and R.E. Prange, Phys. Rev. Lett. **49**, 509 (1982).
[21] D.R. Grempel, R.E. Prange, and S. Fishman, Phys. Rev. A **29**, 1639 (1984).
[22] E.J. Galvez, B.E. Sauer, L. Moorman, P.M. Koch, and D. Richards, Phys. Rev. Lett. **61**, 2011 (1988).
[23] J.E. Bayfield, G. Casati, I. Guarneri, and D.W. Sokol, Phys. Rev. Lett. **63**, 364 (1989).
[24] F.L. Moore, J.C. Robinson, C. Bharucha, P.E. Williams, and M.G. Raizen, Phys. Rev. Lett. **73**, 2974 (1994).
[25] F.M. Izrailev and D.L. Shepelyanskii, Sov. Phys. Dokl. **24**, 996 (1979).
[26] We have used the term ''quantum resonance'' for this phenomenon as it has become standard. This terminology should not be confused with the ''nonlinear resonances'' that already exist in classically chaotic systems and whose overlap leads to the existence of unbounded momentum diffusion in the classical δ-kicked rotor. It has been argued (see, for example, p. 412 of Ref. [13]) that the term ''quantum resonance'' should not be used for the phenomena occurring when $\tau = 4\pi a/b$ because of the potential for confusion, but we have decided to conform to convention.
[27] I. Guarneri (private communication).
[28] R.M. Godun, M.B. d'Arcy, M.K. Oberthaler, G.S. Summy, and K. Burnett, Phys. Rev. A **62**, 013411 (2000).
[29] E. Ott, T.M. Antonsen, Jr., and J.D. Hanson, Phys. Rev. Lett. **53**, 2187 (1984).
[30] I. Guarneri, Lett. Nuovo Cimento Soc. Ital. Fis. **40**, 171 (1984).
[31] M.V. Berry, in *Chaos et Physique Quantique*, Proceedings of the Les Houches Summer School Session LII, edited by M.-J. Giannoni, A. Voros, and J. Zinn-Justin (Elsevier, Amsterdam, 1991), p. 251.
[32] D. Cohen, Phys. Rev. A **44**, 2292 (1991).
[33] S. Dyrting, Phys. Rev. A **53**, 2522 (1996).
[34] R. Blümel, R. Graham, L. Sirko, U. Smilansky, H. Walther, and K. Yamada, Phys. Rev. Lett. **62**, 341 (1989).
[35] H. Ammann, R. Gray, I. Shvarchuck, and N. Christensen, Phys. Rev. Lett. **80**, 4111 (1998).
[36] H. Ammann, R. Gray, I. Shvarchuck, and N. Christensen, J. Phys. B **31**, 2449 (1998).
[37] K. Vant, G. Ball, and N. Christensen, Phys. Rev. E **61**, 5994 (2000).
[38] B.G. Klappauf, W.H. Oskay, D.A. Steck, and M.G. Raizen, Phys. Rev. Lett. **81**, 1203 (1998).
[39] V. Milner, D.A. Steck, W.H. Oskay, and M.G. Raizen, Phys. Rev. E **61**, 7223 (2000).
[40] D.A. Steck, V. Milner, W.H. Oskay, and M.G. Raizen, Phys. Rev. E **62**, 3461 (2000).
[41] J.E. Bayfield and D.W. Sokol, Phys. Rev. Lett. **61**, 2007 (1988).
[42] P.M. Koch, Physica D **83**, 178 (1995).
[43] W.H. Oskay, D.A. Steck, V. Milner, B.G. Klappauf, and M.G. Raizen, Opt. Commun. **179**, 137 (2000).
[44] B.G. Klappauf, W.H. Oskay, D.A. Steck, and M.G. Raizen, Phys. Rev. Lett. **81**, 4044 (1998).
[45] B.G. Klappauf, W.H. Oskay, D.A. Steck, and M.G. Raizen, Physica D **131**, 78 (1999).
[46] C. Cohen-Tannoudji, J. Dupont-Roc, and G. Grynberg, *Atom-Photon Interactions: Basic Processes and Applications* (Wiley, Chichester, 1992).
[47] R. Graham, M. Schlautmann, and P. Zoller, Phys. Rev. A **45**, R19 (1992).
[48] R. Graham and S. Miyazaki, Phys. Rev. A **53**, 2683 (1996).
[49] T. Hogg and B.A. Huberman, Phys. Rev. Lett. **48**, 711 (1982).
[50] T. Hogg and B.A. Huberman, Phys. Rev. A **28**, 22 (1983).
[51] It is possible to view noise introduced in this way as being formally analogous to the making of measurements on the system by detection of the decay photon. Our system undergoes unitary evolution generated by a stochastic Hamiltonian. It has been argued by S. Dyrting and G.J. Milburn, Quantum Semiclassic. Opt. **8**, 541 (1996) that unitary evolution generated by a stochastic Hamiltonian is equivalent to the effect of continuous measurement on the evolution of a quantum system, which is to degrade the signatures of coherent evolution and to restore signatures of classical dynamics. This is consistent with our observations.
[52] D.L. Shepelyansky, Physica D **28**, 103 (1987).
[53] A.J. Daley, A.S. Parkins, R. Leonhardt, and S.M. Tan, e-print quant-ph/0108003.
[54] M.B. d'Arcy, R.M. Godun, M.K. Oberthaler, D. Cassettari, and G.S. Summy, Phys. Rev. Lett. **87**, 074102 (2001).
[55] A.N. Kol'mogorov, Dokl. Akad. Nauk. SSSR **98**, 527 (1954).
[56] V.I. Arnol'd, Russ. Math. Survey **18**, 9 (1963); **18**, 85 (1963).
[57] J. Moser, Nachr. Akad. Wiss. Goett. II, Math-Phys. Kl. **18**, 1 (1962).